Raman spectroscopic study of the mineral xonotlite $Ca_6Si_6O_{17}(OH)_2$ - A component of plaster boards

Ray L. Frost,• Mahen Mahendran, Keerthan Poologanathan and Yunfei Xi

School of Chemistry, Physics and Mechanical Engineering, Science and Engineering Faculty, Queensland University of Technology, GPO Box 2434, Brisbane Queensland 4001, Australia.

Abstract

The mineral xonotlite $Ca_6Si_6O_{17}(OH)_2$ is a crystalline calcium silicate hydrate which is widely used in plaster boards and in many industrial applications. The structure of xonotlite is best described as having a dreierdoppelketten silicate structure, and describes the repeating silicate trimer which forms the silicate chains, and doppel indicating that two chains combine.

Raman bands at 1042 and 1070 cm^{-1} are assigned to the SiO stretching vibrations of linked units of Si_4O_{11} units. Raman bands at 961 and 980 cm^{-1}serve to identify Si_3O_{10} units. The broad Raman band at 862 cm^{-1} is attributed to hydroxyl deformation modes. Intense Raman bands at 593 and 695 cm^{-1} are assigned to OSiO bending vibrations. Intense Raman bands at 3578, 3611, 3627 and 3665 cm^{-1} are assigned to OH stretching vibrations of the OH units in xonotlite. Infrared spectra are in harmony with the Raman spectra. Raman spectroscopy with complimentary infrared spectroscopy enables the characterisation of the building material xonotlite.

• Author to whom correspondence should be addressed (r.frost@qut.edu.au)
P +61 7 3138 2407 F: +61 7 3138 1804

Key words: xonotlite, silicate, Raman spectroscopy, infrared spectroscopy

Introduction

The mineral xonotlite $Ca_6Si_6O_{17}(OH)_2$ is a monoclinic mineral with point group 2/m and consists of needle-like crystals and as flaky fibrous radiating bundles and rosettes [1, 2]. It was first described in 1866 and named for its occurrence in Tetela de Xonotla, Puebla, Mexico. It occurs as veins in serpentinite and contact metamorphism aureoles. The cell data is space group: C2=m, a = 17.03, b = 3.678, c = 7.003 , β = 90:32° and Z = 1. The xonotlite polytypic structure is described by explaining the column build-up along the *b* axis, and the various periodicities along *a* and *c*. This structure may be described as specific polytypisms occurring along 2 directions. The structure of xonotlite is best described as having a dreierdoppelketten silicate structure. This describes the repeating silicate trimer which forms the silicate chains, and doppel indicating that two chains combine. The crystal chemistry of xonotlite is mainly controlled by its four different polytypes [3-5]. XRD results reveal that xonotlite mainly occurs in nature as intergrowths of two up to four polytypes. Xonotlite structure consists of two parallel chains. The defects in the silicate chains of xonotlite offer structural channels accessible for diffusion of ions and water [6]. The defect sites are potential sites for incorporation of foreign ions in the xonotlite structure [3]. These defects in the silicate chains result in pores and xonotlite shows significant porosity [7].

Information on the local structure of xonotlite has been ascertained by NMR spectroscopy [7]. Indeed, NMR allows the types of silica tetrahedra to be determined. Such structure has relevance to the cement industry [8]. The mineral to date is not used as a building material but it does have potential for use in building materials. It may be seen in nuclear waste repositories where the temperature rises significantly [9]. Similarly it may also be found in autoclaved concrete blocks, but it certainly is not seen upon hydration of cement under

47 normal conditions. Some studies of the synthesised analogue of xonotlite and mixtures with
48 MgO with application as binding materials [10]. Black *et al.* systematically investigated the
49 role of synthesis conditions upon the structure and morphology of xonotlite [9]. Starting with
50 a mechano-chemically semicrystalline phase with Ca/Si = 1, these authors prepared a series
51 of xonotlite samples hydrothermally, at temperatures between 200 and 250°C [9]. Other
52 techniques have been used to study xonotlite including XPS, environmental SEM and X-ray
53 diffraction [9, 10].

54

55 Raman studies of cement phases have been forthcoming [11-14]. Some infrared studies of
56 calcium silicates have been undertaken [15-17]. Some Raman spectra of calcium silicates
57 have been collected and a number of the spectra were shown to be dependent upon the
58 number of condensed silica tetrahedra [13]. Such detailed assignment of infrared and Raman
59 bands for a wide range of silicate structures was made by Dowty [18-21].The thermal
60 decomposition of calcium silicates has been measured [22-24]. Xonotlite is readily
61 synthesised. It is often found as components in cements [25, 26]. Xonotlite is used to make
62 reinforced organic polymers. It can be used for the removal of organic polyelectrolytes and
63 their metal complexes by adsorption onto xonotlite. Xonotlite and related minerals can be
64 used for heavy metal uptake for example Nd(II) [25].

65

66 Minerals such as xonotlite and related calcium silicate minerals have wide applications,
67 including insulation boards, refractory boards, fireproof materials, ceiling boards,
68 microporous materials, architectural boards and light weight boards [11, 12]. It is the porosity
69 of xonotlite that is the basis for the industrial applications. In our research, we are adding
70 xonotlite to gypsum in 'gyproc' plaster boards in order to improve the fire resistance of

plaster boards and to raise the temperature at which the plaster boards catch fire. By increasing the content of xonotlite in the gyproc, the plaster boards can be made thinner and lighter. As part of this research, we are interested in determining the spectra of mixtures of xonotlite and gypsum. The objective of this research is to analyse the Raman and infrared spectra of xonotlite and to relate the spectra to the molecular structure of the mineral. In this way we are developing techniques for the analysis of xonotlite mixtures.

Experimental

Mineral

The xonotlite minerals were obtained from The Mineralogical Research Company. The samples originated from (a) Andradite, Hendricksite, Parker Shaft, Franklin, Sussex County, New Jersey (b) Point Sal, near Vandenberg Air Force Base, Santa Barbara County, California and (c) Point Shivery, near Cox's Cove, Bay of Islands, Newfoundland, Canada. Details of the mineral have been published (page 881) [27]. The second xonotlite sample was used for the spectroscopy in this paper. The spectra of all three samples are identical and only one is reported.

Raman spectroscopy

Crystals of xonotlite were placed on a polished metal surface on the stage of an Olympus BHSM microscope, which is equipped with 10x, 20x, and 50x objectives. The microscope is part of a Renishaw 1000 Raman microscope system, which also includes a monochromator, a filter system and a CCD detector (1024 pixels). The Raman spectra were excited by a Spectra-Physics model 127 He-Ne laser producing highly polarised light at 633 nm and

collected at a nominal resolution of 2 cm^{-1} and a precision of ± 1 cm^{-1} in the range between 200 and 4000 cm^{-1}. Repeated acquisitions on the crystals using the highest magnification (50x) were accumulated to improve the signal to noise ratio of the spectra. Xonotlite shows small crystals less than the spatial resolution of the spectrometer and so any Raman measurement is a measurement of more than one crystal. Raman Spectra were calibrated using the 520.5 cm^{-1} line of a silicon wafer. The Raman spectrum of at least 10 crystals was collected to ensure the consistency of the spectra. The Raman spectrum as shown in Figure 1a is an as received spectrum.

Infrared spectroscopy

Infrared spectra were obtained using a Nicolet Nexus 870 FTIR spectrometer with a smart endurance single bounce diamond ATR cell. Spectra over the 4000–525 cm^{-1} range were obtained by the co-addition of 128 scans with a resolution of 4 cm^{-1} and a mirror velocity of 0.6329 cm/s. Spectra were co-added to improve the signal to noise ratio.

Spectral manipulation such as baseline correction/adjustment and smoothing were performed using the Spectracalc software package GRAMS (Galactic Industries Corporation, NH, USA). Band component analysis was undertaken using the Jandel 'Peakfit' software package that enabled the type of fitting function to be selected and allows specific parameters to be fixed or varied accordingly. Band fitting was undertaken using a Lorentzian-Gaussian cross-product function with the minimum number of component bands used for the fitting process. The Lorentzian-Gaussian ratio was maintained at values greater than 0.7 and fitting was undertaken until reproducible results were obtained with squared correlations of r^2 greater than 0.995.

118

119 **Results and Discussion**

120 The Raman spectrum of xonotlite in the 100 to 4000 cm^{-1} range and infrared spectrum of
121 xonotlite in the 500 to 4000 cm^{-1} range are displayed in Figure1. These spectra illustrate the
122 relative intensities of the bands and the position of the peaks. It is obvious that there are large
123 sections of the spectra where no intensity is observed. Thus, the spectra are subdivided into
124 sections dependent upon the particular vibration being studied. The Raman spectrum of
125 xonotlite in the 800 to 1400 cm^{-1} is reported in Figure 2a and the infrared spectrum in the 500
126 to 1300 cm^{-1} range in Figure 2b.

127

128 The structure of xonotlite is such that a double chain is formed by combining two single
129 chains side by side so that all the right sided tetrahedrons of the left chain are linked by an
130 oxygen to the left sided tetrahedrons of the right chain [3]. The structure of xonotlite is best
131 described as having a dreierdoppelketten silicate structure, and describes the repeating silicate
132 trimer which forms the silicate chains, and doppel indicating that two chains combine. The
133 extra shared oxygen for every four silicons reduces the ratio of oxygen to silicons to 11:4.
134 Dowty calculated the band positions for the different ideal silicate units. Dowty showed that
135 the -SiO_3 units had a unique band position of 1025 cm^{-1} [21] (see Figures 2 and 4 of this
136 reference). Xonotlite has chains of linked units of Si_4O_{11}. Dowty calculated the Raman
137 spectrum for these type of silicate networks and predicted two bands at around 1040 and
138 1070 cm^{-1} with an additional band at around 600 cm^{-1}. In Figure 2a, we observe two bands at
139 1042 and 1070 cm^{-1} in harmony with Dowty's predictions. Two other Raman bands are
140 observed at 961 and 980 cm^{-1}. These Raman bands identify Si_3O_{10} units. A significantly
141 broader band is observed at 862 cm^{-1}. This band is not associated with siloxane units but is

attributed to hydroxyl deformation modes. The 1042 cm^{-1} Raman band is not observed in the infrared spectrum (Figure 2b). This indicates that the vibration contains a centre of symmetry. Infrared bands are observed at 1072 and 1 198 cm^{-1}. This latter band is not observed in the Raman spectrum. Strong infrared bands are observed at 928 and 972 cm^{-1}. Dowty calculated the position of infrared bands for silicate structures and also showed measured spectra of the equivalent theoretical system. The infrared bands shown were broad. In this work the infrared bands of xonotlite are sharp and easily resolved. Garbev *et al.* [28] reported the Raman spectra of a series of calcium silicate hydrate compounds with varying Ca/Si ratios. There is some resemblance between the spectra of this reference (see Figure 3 of this reference) and our spectra. However it must be pointed out that the compounds synthesised by Black *et al.* were calcium silicates hydrates. In comparison, xonotlite is a hydroxy calcium silicate. Richardson *et al.* [14] published a review of cement phases and their characterisation of calcium silicate phases by a number of techniques including Raman spectroscopy.

The Raman spectrum of xonotlite in the 300 to 800 cm^{-1} region and in the 100 to 300 cm^{-1} region are displayed in Figure 3. Two intense sharp Raman bands are observed at 593 and 695 cm^{-1}. The Raman band at 695 cm^{-1} is assigned to the OSiO bending vibrations of the Si_3O_{10} units. The equivalent bands in the infrared spectrum are observed at 607, 634, 653 and 669 cm^{-1} (Figure 2b). These bands are assigned to OSiO bending modes. Black *et al.* [29] reported the spectra of hydrated calcium silicates and reported a strong Raman band at 670 cm^{-1} and attributed this band to a Si-O-Si symmetric bending mode. The band is in a higher wavenumber position than for a single silicate chain [14]. This difference is related to the differences in the structures between xonotlite and the hydrated calcium silicates. The Raman band at 593 cm^{-1} is assigned to the OSiO out-of-plane bending vibrations of the

Si_4O_{11} units. A series of low intensity Raman bands are observed at 304, 335, 369, 393, 421 and 445 cm^{-1}. These bands are considered to be associated with Ca-O bonds. Two Raman bands are observed at 505 and 524 cm^{-1}. Bands in these positions are assigned to the OSiO bending modes of SiO_2 units [21]. Some intense Raman bands are observed in the far low wavenumber region. Strong Raman bands are observed at 135, 205 and 234 cm^{-1} with bands of lower intensity at 158, 259 and 271 cm^{-1}. These bands are simply described as lattice vibrations. It is suggested that these bands are related to the OH units and the hydrogen bonding to the silicate units.

The Raman spectrum of xonotlite in the 2600 and 3800 cm^{-1} and the infrared spectrum in the 2400 to 3800 cm^{-1} are reported in Figure 4. Intense bands are observed in both the Raman and infrared spectrum. Intense Raman bands are observed at 3578, 3611, 3627 and 3665 cm^{-1}. These bands are assigned to the OH stretching bands of the OH units in xonotlite. Some low intensity bands are observed at 2909, 3303 and 3528 cm^{-1}. These bands are attributed to water hydrogen bonded to the OH units of xonotlite. These bands attributed to water stretching vibrations show much greater intensity in the infrared spectrum with resolved infrared bands observed at 2907, 3529, 3459 and 3576 cm^{-1}. The range of peak positions provides evidence for a range of hydrogen bond strengths. Both Raman and infrared bands at around 2909 cm^{-1} are attributed to strong hydrogen bonding. The hydrogen bond distance is short. The infrared band at 3529 cm^{-1} is attributed to water stretching vibration with intermediate hydrogen bond strength. Such a range of hydrogen bond strengths is also reflected in the water bending modes (Figure 5) where two bands are resolved at 1603 and 1660 cm^{-1}. This latter band is attributed to the water bending modes of water involved in strong hydrogen bonding. The band at 1603 cm^{-1} is assigned to the water bending mode of water involved in weak hydrogen bonding.

Conclusions

Xonotlite as a building material has many and varied applications which are based upon the inherent properties of xonotlite including porosity, thermal insulation and thermal decomposition temperature. In order to raise the on-set combustion temperature of plaster boards new types of plaster boards are made by combining gypsum with xonotlite. As part of this research, we have undertaken a vibrational spectroscopic study of xonotlite to determine the characteristic bands of this mineral.

The Raman spectrum of xonotlite is characterised by intense sharp bands at 961, 980, 1042 and 1070 cm^{-1}. These bands are assigned to the SiO stretching vibrations of the Si_4O_{11} and Si_3O_{10} units. Intense Raman bands at 593 and 695 cm^{-1} are assigned to OSiO bending vibrations. The intense Raman band profile centred upon 3611 cm^{-1} is attributed to the OH stretching vibrations of the OH units in the xonotlite structure. The mineral xonotlite is well and truly characterised by its Raman spectrum. Further, Raman spectroscopy offers a technique for the study of xonotlite and its admixtures including gypsum.

Acknowledgments

The financial and infra-structure support of the School of Chemistry, Physics and Mechanical Engineering, Science and Engineering Faculty, Queensland University of Technology, is gratefully acknowledged. The Australian Research Council (ARC) is thanked for funding the instrumentation.

References

[1] Mamedov, K. S., Belov, N. V., Structure of xonotlite,Doklady Akademii Nauk SSSR 104 (1955) 615-618.

[2] Mamedov, K. S., Belov, N. V., Crystal structure of the minerals of the wollastonite group. I. Structure of xonotlite,Zapiski Vserossiiskogo Mineralogicheskogo Obshchestva 85 (1956) 13-38.

[3] Bernstein, S., Fehr, K. T., Hochleitner, R., Crystal chemistry of Xonotlite Ca6Si6O17(OH)2. Part I: determination of polytypes using X-ray Powder Diffraction (XRPD),Neues Jahrbuch fuer Mineralogie, Abhandlungen 186 (2009) 153-162.

[4] Churakov, S. V., Mandaliev, P., Structure of the hydrogen bonds and silica defects in the tetrahedral double chain of xonotlite,Cement and Concrete Research 38 (2008) 300-311.

[5] Hejny, C., Armbruster, T., Polytypism in xonotlite Ca6Si6O17(OH)2,Zeitschrift fuer Kristallographie 216 (2001) 396-408.

[6] Hejny, C., Armbruster, T., Structure modeling and identification of xonotlite polytypes,Applied Mineralogy: In Research, Economy, Technology, Ecology and Culture, Proceedings of the International Congress on Applied Mineralogy, 6th, Goettingen, Germany, July 17-19, 2 2 (2000) 795-797.

[7] Grimmer, A. R., Wieker, W., Determination of the type of water bonding in xonotlite 6CaO.6SiO2.H2O,Zeitschrift fuer Anorganische und Allgemeine Chemie 384 (1971) 34-42.

[8] Lippmaa, E., Maegi, M., Samoson, A., Engelhardt, G., Grimmer, A. R., Structural studies of silicates by solid-state high-resolution silicon-29 NMR,Journal of the American Chemical Society 102 (1980) 4889-4893.

[9] Black, L., Garbev, K., Stumm, A., Structure, bonding and morphology of hydrothermally synthesised xonotlite,Advances in Applied Ceramics 108 (2009) 137-144.

[10] Milestone, N. B., Ahari, K. G., Hydrothermal processing of xonotlite based compositions,Advances in Applied Ceramics 106 (2007) 302-308.

[11] Black, L., Raman spectroscopy of cementitious materials,Spectroscopic Properties of Inorganic and Organometallic Compounds 40 (2009) 72-127.

[12] Black, L., Breen, C., Yarwood, J., Phipps, J., Maitland, G., In situ Raman analysis of hydrating C3A and C4AF pastes in presence and absence of sulphate,Advances in Applied Ceramics 105 (2006) 209-216.

[13] Pilz, W., Raman spectra of silicates,Acta Physica Hungarica 61 (1987) 27-30.

[14] Richardson, I. G., Skibsted, J., Black, L., Kirkpatrick, R. J., Characterisation of cement hydrate phases by TEM, NMR and raman spectroscopy,Advances in Cement Research 22 (2010) 233-248.

[15] Henning, O., Gerstner, B., Infrared and x-ray analytical characterization of natural and synthetic calcium silicate hydrates,Wissenschaftliche Zeitschrift der Hochschule fuer Architektur und Bauwesen Weimar 19 (1972) 287-293.

[16] Krylov, G. M., Priev, Y. M., Infrared spectrometric study of xonotlite,Doklady Akademii Nauk UzSSR (1959) 25-27.

[17] Krylov, G. M., Sirotenko, G. F., Infrared spectra of xonotlite, hillebrandite, and tobermorite,Doklady Akademii Nauk UzSSR (1961) 41-44.

[18] Ancillotti, L., Castellucci, E. M., Becucci, M., A combined Raman-LIBS spectrometer: toward a mobile atomic and molecular analytical tool for in situ applications,Proceedings of SPIE-The International Society for Optical Engineering 5850 (2005) 182-189.

[19] Dowty, E., Vibrational interactions of tetrahedra in silicate glasses and crystals. III. Calculations on simple sodium and lithium silicates, thortveitite and rankinite,Physics and Chemistry of Minerals 14 (1987) 542-552.
[20] Dowty, E., Vibrational interactions of tetrahedra in silicate glasses and crystals: II. Calculations on melilites, pyroxenes, silica polymorphs and feldspars,Physics and Chemistry of Minerals 14 (1987) 122-138.
[21] Dowty, E., Vibrational interactions of tetrahedra in silicate glasses and crystals: I. Calculations on ideal silicate-aluminate-germanate structural units,Physics and Chemistry of Minerals 14 (1987) 80-93.
[22] Okada, Y., Shibasaki, H., Masuda, T., Thermal decomposition of calcium silicate hydrates,Onoda Kenkyu Hokoku 45 (1994) 126-141.
[23] Winkler, A., Wieker, W., Thermal behavior of 11 Å tobermorite,Zeitschrift fuer Chemie 18 (1978) 375-376.
[24] Zadov, A. E., Chukanov, N. V., Organova, N. I., Kuz'mina, O. V., Belokovskii, D. I., Litsarev, M. A., Nechai, V. G., Sokolovskii, F. S., Hydration, dehydration and thermal transformation of tobermorite family minerals,Zapiski Vserossiiskogo Mineralogicheskogo Obshchestva 130 (2001) 26-40.
[25] Komarneni, S., Roy, D. M., Kumar, A., Tuff-cement or concrete interactions in the repository environment,Materials Research Society Symposium Proceedings 44 (1985) 927-934.
[26] Noma, H., Adachi, Y., Yamada, H., Matsuda, Y., Yokoyama, T., Formation mechanism of xonotlite from poorly-crystalline calcium silicate hydrate (C-S-H),International Ceramic Monographs 2 (1996) 2450-2458.
[27] Anthony, J. W., Bideaux, R. A., Bladh, K. W., Nichols, M. C., Silica, Silicates, Mineral data Publishing, Tucson, Arizona, 1995.
[28] Garbev, K., Stemmermann, P., Black, L., Breen, C., Yarwood, J., Gasharova, B., Structural features of C-S-H(I) and its carbonation in air - a Raman spectroscopic study. Part I: Fresh phases,Journal of the American Ceramic Society 90 (2007) 900-907.
[29] Black, L., Breen, C., Yarwood, J., Garbev, K., Stemmermann, P., Gasharova, B., Structural features of C-S-H(I) and its carbonation in air - a Raman spectroscopic study. Part II: carbonated phases,Journal of the American Ceramic Society 90 (2007) 908-917.

295 **List of Figures**

305

306

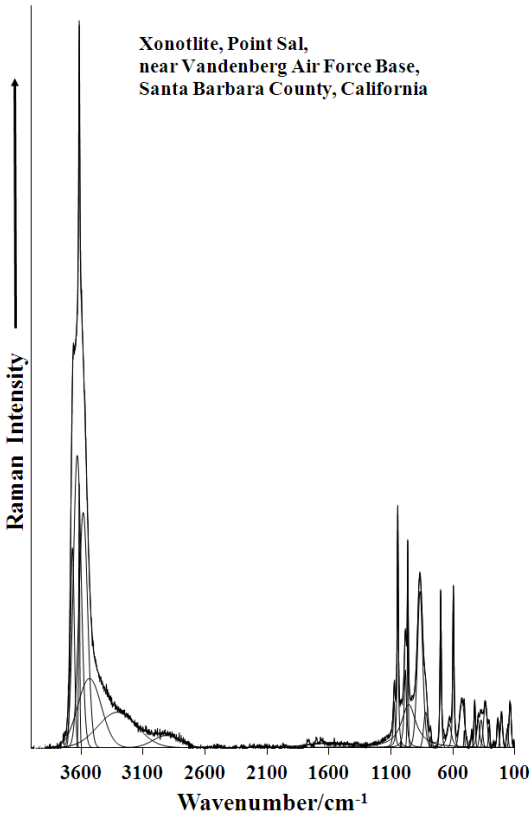

Figure 1a

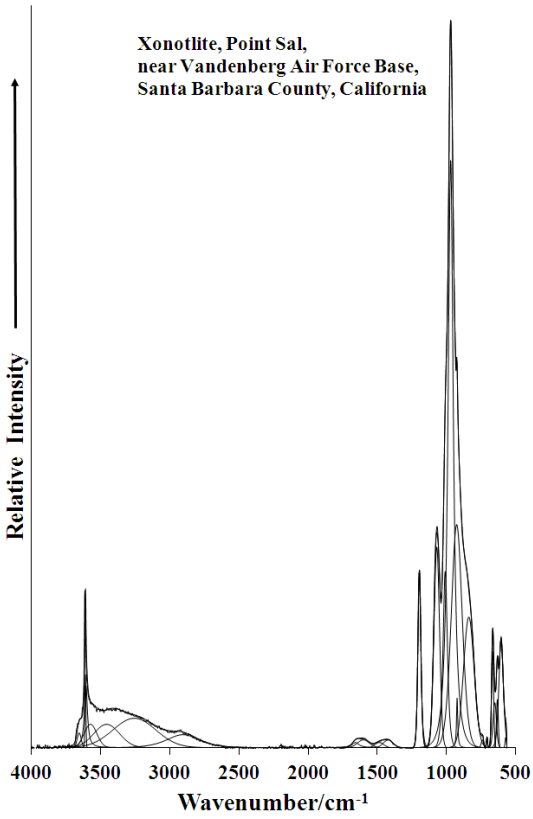

Figure 1b

307

308

309

310

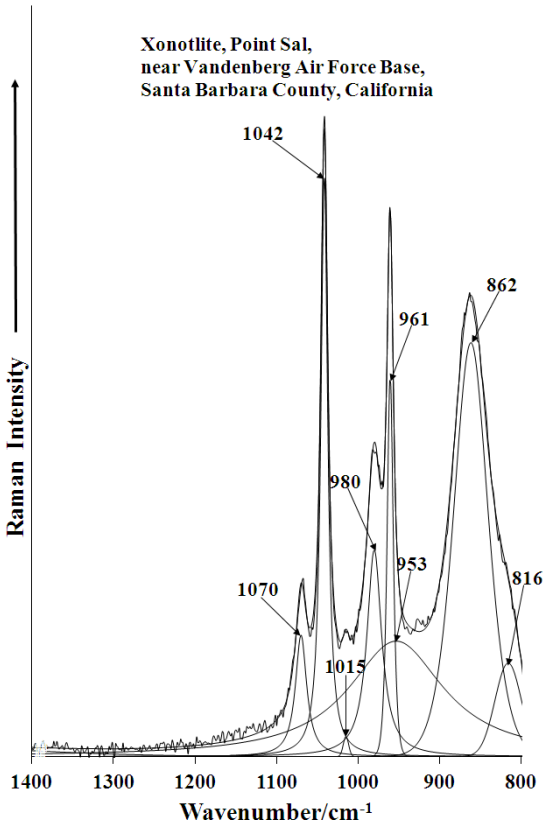

Figure 2a

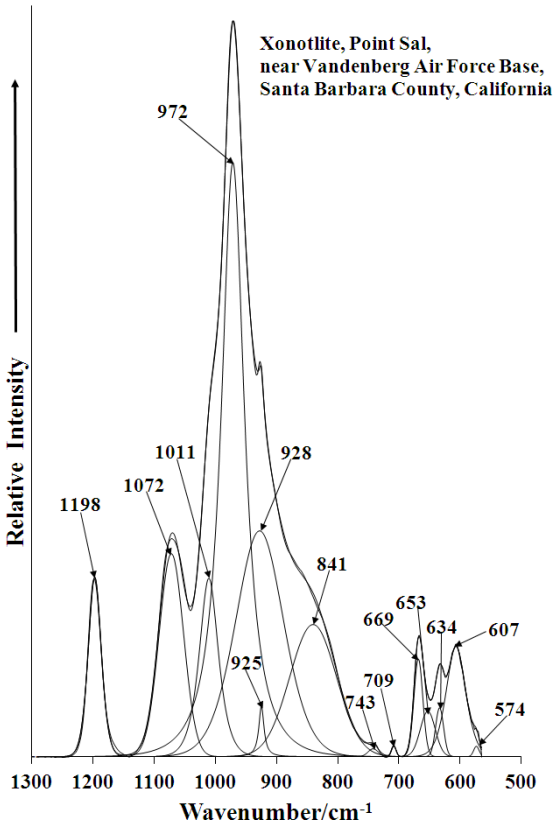

Figure 2b

311

312

313

314

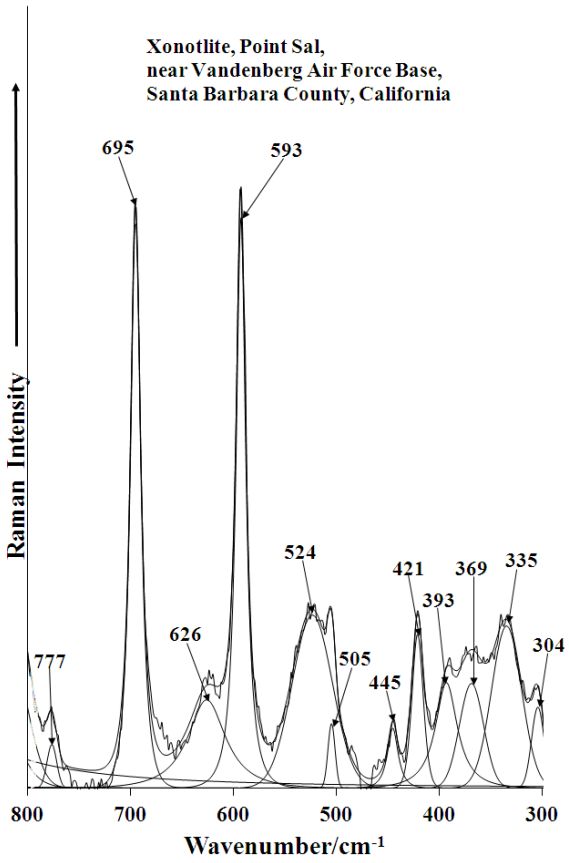

Figure 3a

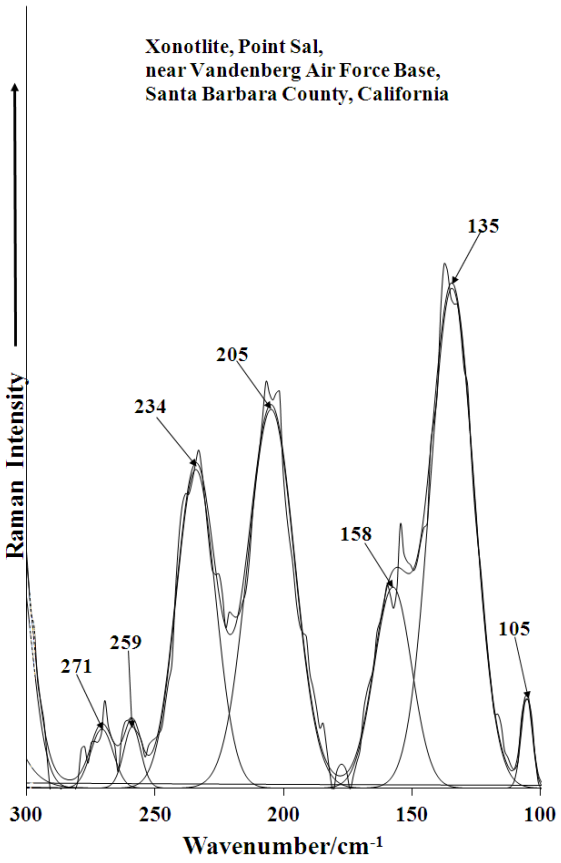

Figure 3b

315

316

317

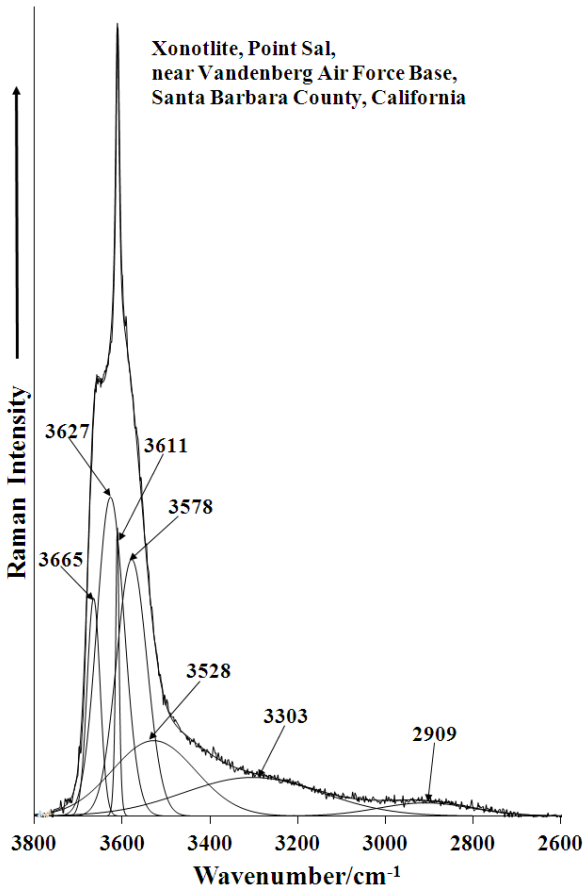

Figure 4a

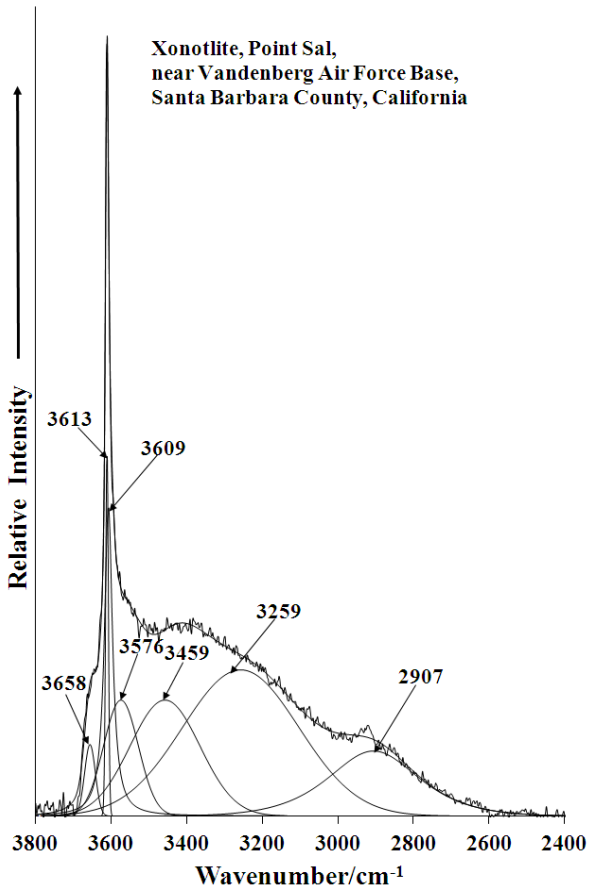

Figure 4b

318

319

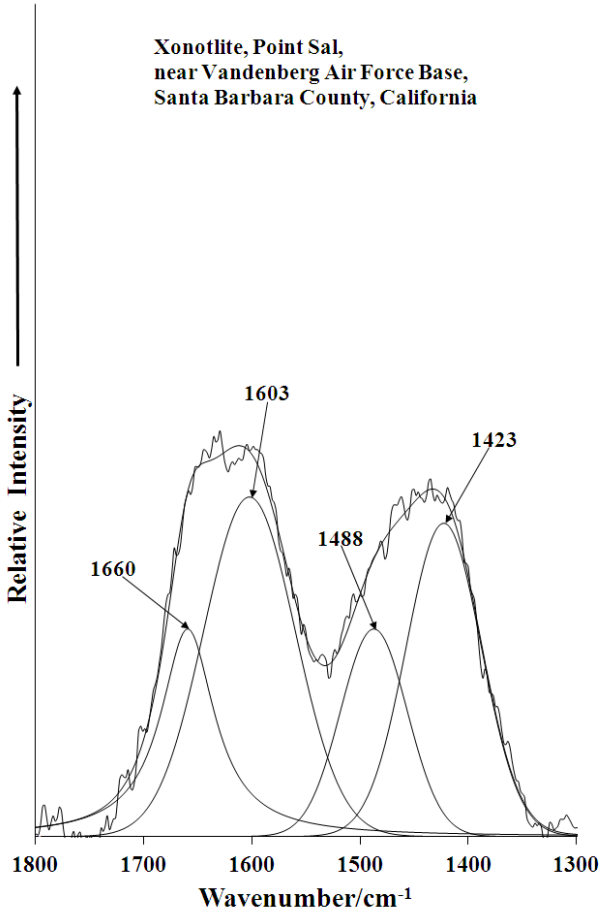

320

321 **Figure 5**